

AMPTIAC

A Facsimile Report

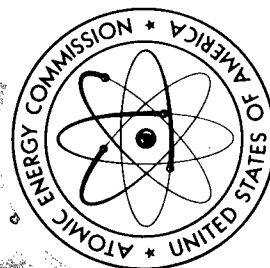
Reproduced From
Best Available Copy

Reproduced by
**UNITED STATES
ATOMIC ENERGY COMMISSION**
Division of Technical Information

P.O. Box 62 Oak Ridge, Tennessee 37830

DISTRIBUTION STATEMENT A
Approved for Public Release
Distribution Unlimited

DTIC QUALITY INSPECTED 4



20000907 193

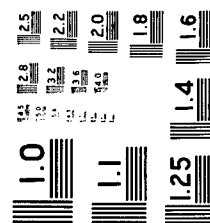
VERL-17449

69791

1 OF 1

UCRL

17449



MICROCOPY RESOLUTION TEST CHART
NATIONAL BUREAU OF STANDARDS - 1963

UCRL-17449

-iii-

UCRL-7449

COSTS PRICES

H.Q. \$ 3.00; MN 65

UNIVERSITY OF CALIFORNIA
Lawrence Radiation Laboratory
Berkeley, California

AEC Contract No. W-7405-eng-48

THE LOW TEMPERATURE THERMALLY ACTIVATED DEFORMATION
MECHANISMS FOR BCC MAGNESIUM-LITHIUM-ALUMINUM ALLOY

Contents

Abstract	v
I. Introduction	1
II. Dorn and Rajnak's Model of Peierls' Mechanism	3
III. Experimental Procedure	6
IV. Experimental Results and Discussion	7
V. Activation Volume	11
VI. Activation Energy of Pairs of Kinks	14
VII. Line Tension of Dislocation Situated at the Peierls Valley	16
VIII. Experimental Value of the Number of Dislocations per Unit Length (ρ_L)	17
IX. Conclusions	18
Appendix I	19
Acknowledgement	21
References	22

THE LOW TEMPERATURE THERMALLY ACTIVATED DEFORMATION
MECHANISMS FOR BCC MAGNESIUM-LITHIUM-ALUMINUM ALLOY

Mohamed Osama Abo-el-Fotch

(M. S. thesis)

March 1967

LEGAL NOTICE

This report was prepared as an account of Government sponsored work. Neither the United States, nor the Commission, nor any person acting on behalf of the Commission, makes any warranty or representation, expressed or implied, with respect to the accuracy, completeness, or usefulness of the information contained herein or to the use of any information, apparatus, method, or process disclosed in this report may not infringe privately owned rights, or use of any information with respect to the use of, or for damages resulting from the use of, any information disclosed herein.

As used in the above, "person acting on behalf of the Commission" includes any employee or contractor of the Commission, or employee of such contractor, in the extent that he or she is authorized by the Commission or employee of such contractor to prepare, disseminate, or provide access to, any information derived from the employment or contract with the Commission, or its employment with such contractor.

DISTRIBUTION OF THIS DOCUMENT IS UNLIMITED

THE LOW TEMPERATURE THERMALLY ACTIVATED DEFORMATION MECHANISMS
FOR FCC MAGNESIUM-LITHIUM-ALUMINUM ALLOY

Mohamed Sami Abo-el-Fotoh

Lawrence Materials Research Division, Lawrence Radiation Laboratory,
and Department of Mineral Technology, College of Engineering,
University of California, Berkeley, California

March, 1967

ABSTRACT

The effect of strain rate and temperature on the flow stress was investigated in a polycrystalline magnesium-14 wt. % lithium-1.5 wt. % aluminum alloy. Whereas the flow stress increased only slightly as the temperature was decreased from room temperature to about 115°K, a rapid increase in the flow stress was obtained with yet greater decreases in temperature from about 115° to 20°K. The strong temperature and strain rate dependence of the flow stress below 115°K was interpreted in terms of the Dorn-Raynax theory of the Peierls mechanism when the deformation is controlled by the rate of nucleation of pairs of kinks. Above 115°K, an athermal mechanism is operative.

I. INTRODUCTION

This investigation was undertaken for the purpose of elucidating the rate-controlling mechanism for slip in polycrystalline aggregates of b.c.c. magnesium, 14 wt. % Al, 1.0 - 1.5 wt. % Al alloy as part of a more general program of study on the plastic behavior of b.c.c. metals, alloys, and intermetallic compounds. The flow stress of this alloy depends strongly on temperature and strain rate over the low temperature region (below about 115°K). A basic understanding of its mechanical behavior necessitates a thorough investigation of the rate controlling mechanisms of the mobile dislocations. The following thermally-activated dislocation mechanisms have been proposed:

- (a) Interaction of dislocations with interstitial impurity atoms or with solute atoms in general,
- (b) Overcoming the Peierls-Nabarro stress,
- (c) Resistance to the motion of dislocations due to jogs on screw dislocations,
- (d) Overcoming interstitial precipitates,
- (e) Cross-slip.

It was concluded by Dorn and Raynax,¹ Conrad,² and Christian and Masters,³ that in b.c.c. metals the overcoming of the Peierls-Nabarro stress which arises from the variations in bond energies of atoms in the dislocation core as it is displaced, is the most probable rate controlling mechanism. Several models of the Peierls mechanism have been formulated. Experimental results obtained from the deformation of Mo, Nb, Ta, Ag₃C, Ag₃Al and Fe-2 1/2 % Mn alloy have been successfully explained by the Dorn-Raynax model of nucleation of kink pairs.

Start

The purpose of this work was to investigate the mechanical behavior of superlattice aggregates of magnesium, 14 wt. % Al, and 1.0 - 1.55 Al alloy at low temperatures and to correlate the experimental results with the Peierls mechanism using the Dorn and Rajnak model.

It will be shown that the strong dependence of temperature and strain rate can be satisfactorily explained by the rate of nucleation of pairs of kinks on dislocations involved in the Peierls mechanism for plastic deformation.

to p.v

II. DORN AND RAJNAK'S MODEL OF PEIERLS' MECHANISM

A straight dislocation line has its lowest energy when it lies in a potential valley parallel to lines of closest packing of atoms on the slip plane. When such a straight dislocation line moves from one valley toward the next, the atoms in the vicinity of the core of the dislocation change their positions and bond angles, causing the energy of the dislocation to increase. The core energy of the dislocation is assumed to reach a maximum value midway between the two adjacent valleys. Any additional small displacement will cause the dislocation to fall down the hill into the next valley which is another minimum energy position for the dislocation. The shear stress necessary to promote such forward motion of the dislocation at the absolute zero is known as the Peierls stress τ_p .

A forward motion of such kind can be achieved by the nucleation of a pair of kinks under the influence of an applied stress and a thermal fluctuation. When a stress τ^* less than τ_p is applied to the slip plane in the direction of the Burger's vector, the dislocation will move as shown in Fig. 1, from its original position $A_0B_0C_0$ in the valley to a parallel position $A'B'C'$ part way up the Peierls hill. No further motion will occur at the absolute zero. At higher temperatures, thermal fluctuations cause the dislocation to vibrate about its mean position. When a local thermal fluctuation is sufficiently energetic, a dislocation loop $A_0B_0C_0$ of a critical size is produced which no longer returns to its original position. For all configurations exceeding the critical one, the two kink segments $A'B'$ and $B'C'$ will move apart under the action of the applied stress, resulting in a forward motion of the dislocation by a displacement,

a , equal to the periodicity of the rows of closely spaced atoms on the slip plane.

Dorn and Rajnak applied the suggestion of Friedel that the major factor involved in kink nucleation is the additional energy due to the curvature in the length of the dislocation line. γ_y was taken to be the energy per unit length of a dislocation where the y direction was defined as shown in Fig. 1. Therefore, the line energy was assumed to be a periodic function of y with a period a . The minor variations of the line energy with curvature and proportions of edge and screw dislocations were neglected. Furthermore, although the exact shape of the Peierls hill was not known, it was assumed by Dorn and Rajnak to be approximated by:

$$\gamma(y) = \frac{\gamma_0^2}{2} + \frac{\gamma_0^2}{2} \left(\frac{y}{a} + \cos \frac{2\pi y}{a} - \frac{y}{a} \cos \frac{4\pi y}{a} \right) \quad (1)$$

where γ_0 and γ_0^2 are the energies per unit length of a dislocation lying at the top and bottom of the Peierls hill, respectively, and a is a hill shape factor that was assumed to vary between -1 and +1.

Under a stress τ the stable equilibrium position of an infinitely long dislocation is $y = y_0$. The difference in energy of a displaced dislocation line (AEC, Fig. 1) and that of the corresponding straight dislocation line lying along $y = y_0$ is given by

$$U = \int_{-\infty}^{\infty} \left(\gamma(y) \sqrt{1 + \left(\frac{dy}{dx} \right)^2} - \gamma(y_0) \right) dx \quad (2)$$

where the first two terms of the integrand are the line energies of the

dislocation in the two positions, and the third term gives the extra work done by the applied stress τ in displacing the dislocation from y_0 to y . The critical energy for nucleating one pair of kinks was calculated by using Euler's conditions for minimizing the energy. Upon numerical integration of the above equations, Dorn and Rajnak were able to obtain a universal relationship between $\dot{\gamma}/2U_K$ and τ/τ_p (U_K is the kink energy), from which relationship could be derived between the activation volume and the applied stress, and between the velocity of the dislocation and the applied stress.

III. EXPERIMENTAL PROCEDURE

The material used in this investigation consisted of a b.c.c.

magnesium, 14 wt.% Al 1.0 - 1.5 wt.% Al alloy. Tensile specimens 0.2"

in dia having 2" long gauge section were machined from the as received

1 in x 6 in x 12 in sheets, annealed under argon at 3000° (1500°C)

for 4 hours to remove all the deformation put into the specimen during

the machining and finally etched in dilute hydrochloric acid solution to remove the thin oxide films.

All tensile tests were performed at strain rates of $3.13 \times 10^{-3} \text{ sec}^{-1}$

and $3.13 \times 10^{-5} \text{ sec}^{-1}$ on an Instron testing machine in controlled temperature

baths. The temperature variation was controlled within $\pm 2^\circ\text{K}$ of the

recorded value. For testing temperatures below 77°C , a specially designed

Drystat was used.

IV. EXPERIMENTAL RESULTS AND DISCUSSION

The dependence of flow stress on temperature and strain rate:

The applied shear stress that is required to cause plastic flow is given by:

$$\tau = \tau^* + \tau_A \quad (2)$$

where τ is the applied shear stress, and τ^* is the stress required to aid the thermal activation of the rate controlling mechanism and therefore decreases precipitously as T increases. τ_A is the stress necessary to overcome any athermal barriers and therefore it decreases only modestly as the temperature increases, usually parallel to the shear modulus of elasticity.

The primary interests of this work lie in the temperature and strain rate dependence of the dependence of the thermally activated component of the stress. The results are shown in Fig. 2 and Fig. 3.

The increasing flow stress with increasing strain rate as well as decreasing temperature attests to the fact that the operative deformation mechanism is thermally activated. Tests below 20°K were not performed due to the difficulties in controlling the stability of temperature.

The curves in Figs. 2 and 3 were extrapolated to 0°K . Over the lower ranges of test temperatures, where the flow stress decreases rapidly from 20°K to 115°K for both strain rates, the thermally activated component τ^* of the stress was calculated from the relationship:

$$\tau^* = \tau_T - \tau_{235} \frac{G(T)}{G(235)} \quad (4)$$

where τ_a is the total resolved shear stress for flow at temperature $T^{\circ}K$, and the term $\frac{G(T)}{G(235)}$ is the total back stress, corrected for the change in shear modulus with temperature. The variation of shear modulus with temperature was calculated from data obtained by J. Trivisonno and S. Smith, Fig. 4. Values of τ^* , which are now corrected for specimen variation in τ_a , are shown in Fig. 3 for two strain rates.

For a thermally activated mechanism, the plastic strain rate is given by (see Appendix 1):

$$\dot{\gamma} = \frac{\rho \text{Lab}^2 v}{2\pi^2} e^{-\frac{U_n(\tau^*)}{kT}} \quad (5)$$

where ρ = density of mobile dislocations

a = the distance between Peierls' valleys

b = Burger's vector

v = the Debye frequency

L = the mean length swept out by a pair of kinks once nucleation occurs in that length

w = width of a pair of kinks at the saddle point free energy configuration

$U_n(\tau^*)$ = Saddle point free energy for nucleation of pairs of kinks

k = Boltzmann constant

T = absolute temperature

When the testing temperature reaches a critical temperature, T_c , for a given strain rate, the thermally activated component of the stress τ^* becomes zero and the thermal energy that needs to be supplied to nucleate

a pair of kinks is just $2U_n$, where U_n is the energy of a single kink. Therefore, at $T = T_c$

$$\dot{\gamma} = \frac{\rho \text{Lab}^2 v}{2\pi^2} e^{-\frac{2U_n(T_c)}{kT_c}} \quad (6)$$

The theory of Dorn and Rajnak predicts a universal relationship between $U_n/2U_n$, where U_n is the saddle-point free energy for nucleation of a pair of kinks and U_n is the kink energy, and τ^*/τ_p . But as shown by Dorn and Rajnak, to a very good approximation $w = v_c$, where v_c is the critical width of a pair of kinks and therefore, as shown by Eqs. (5) and (6),

$$\frac{U_n(T)}{2U_n(T)} = \frac{U_n(T)}{2U_n(T_c)} \frac{G(T)}{G(T_c)} = \frac{T_c}{T} \frac{G(T)}{G(T_c)} \quad (7)$$

It is the purpose of this work to correlate the relationship predicted by the theory with that obtained from the experimental results. The expected theoretical trends as shown by the solid curves in Fig. 5 are in excellent agreement with the experimental results at low temperatures (from $20^{\circ}K$ to $115^{\circ}K$ for $\dot{\gamma} = 3.13 \times 10^{-5} \text{ sec}^{-1}$ and from $20^{\circ}K$ to $180^{\circ}K$ for $\dot{\gamma} = 3.13 \times 10^{-3} \text{ sec}^{-1}$) and it appears to agree best with the curve representing $\alpha = +1$. At higher temperatures an athermal mechanism is operative. Experimental results are presented in Table 1.

Table 1. Strain rate, temperature dependence of the thermally activated component of the flow stress.

T, °C	$\dot{\gamma} = 3.13 \times 10^{-5} \text{ sec}^{-1}$		$\dot{\gamma} = 3.13 \times 10^{-3} \text{ sec}^{-1}$
	$\tau^* \times 10^{-8} \text{ dynes/cm}^2$		
19			6.71
20	5.97		
25			4.32
30	2.99		
35	1.43		2.55
38	0.76		1.56
40	0.29		1.15
45	0	0.32	
46	0	0	
53	0	0.05	
57	0.09	0.12	
60	0	0.21	

τ_p extrapolated = $8.40 \times 10^8 \text{ dynes/cm}^2$

The critical temperature at $\dot{\gamma}_1 = 3.13 \times 10^{-5} \text{ sec}^{-1}$. $T_{c1} = 115^\circ\text{K}$

The critical temperature at $\dot{\gamma}_2 = 3.13 \times 10^{-3} \text{ sec}^{-1}$. $T_{c2} = 180^\circ\text{K}$

V. ACTIVATION VOLUME

The activation volume is defined by:

$$V = - \left(\frac{\partial \tau}{\partial \ln \dot{\gamma}} \right)_T = kT \left(\frac{\partial \ln \dot{\gamma}}{\partial \ln \tau} \right)_T = kT \left(\frac{\partial \ln \dot{\gamma}}{\partial \ln \tau} \right)_T \quad (2)$$

The activation volume approximates the product of the Burger's vector and the area swept out during the nucleation of the critical loop (Fig. 1). The Peierls mechanism has a unique low value of the activation volume (usually ranging from 500 to 5000). The activation volume remains constant and is unaffected by increasing the strain. These properties of the activation volume are the most reliable verification of the Peierls mechanism. The properties of the activation volume of the other suggested mechanisms are shown in Table 2. The experimental activation volumes are obtained by the effect of small changes in strain rate on the flow stress. A quantity δ is defined as:

$$\delta = \left(\frac{\partial \ln \tau}{\partial \ln \dot{\gamma}} \right)_T \quad (9)$$

kT is defined as the apparent activation volume:

$$V_a = \delta kT = kT \left(\frac{\partial \ln \tau}{\partial \ln \dot{\gamma}} \right)_T \quad (10)$$

For the Peierls mechanism (Eq. (5)), this becomes

$$V_a = kT \left(\frac{\partial \ln \tau}{\partial \ln \dot{\gamma}} \right)_T = 2kT \left(\frac{\partial \ln \tau}{\partial \ln \dot{\gamma}} \right)_T = \frac{2b^2}{\delta \tau} \quad (11)$$

Table 2. The properties of the activation volume of other suggested mechanisms.

Mechanism	Properties
Interaction of dislocations with interstitial impurity atoms or with solute atoms in general. 10-13	1. V_a depends on interstitial content. Higher values of V_a (probably up to 1000b ³).
Persistence to the motion of dislocations due to loops on screw dislocations. 11-16	1. V_a depends on the structure. 2. Athermal at low temperatures thermally activated at relatively high temperature.
Overcoming interstitial precipitates. 17	3. $V_a = 2b_j^2$ (2_j = length of jog). 1. $V_a = 2b_j^2$ (2_j = length of the precipitates). 2. V_a varies with the impurity content.
Overcoming dislocations. 18	1. High activation volume (of the order of 700b ³ - 800b ³).

The negative of the last term of Eq. (11) is the theoretical activation volume V^* . The theoretical activation volume V^* can be rewritten as:

$$V^* = - \frac{\partial U_a}{\partial \tau^*} = - \frac{2U_a(C)}{\tau^*} \frac{\partial \left(\frac{U_a}{2U_a(C)} \right)}{\partial \left(\frac{\tau^*}{\tau_0} \right)} \quad (12)$$

Whereas the term containing w in Eq. (11) is always negligibly small, the apparent activation volume can be slightly larger than the theoretical one, V^* , as a result of the possible increase in the dislocation density, ρ , as the stress is increased. Consequently, when the Peierls mechanism is operative, V_a closely follows the trends of V^* . Fig. 6 shows the apparent activation volume as a function of stress, the low values of V_a in terms of b^3 agree very well with the low activation volume as predicted by the Peierls mechanism. Figure 7 also shows the relatively constant value of the apparent activation volume with increasing strain. The theoretical plot for the activation volume as a function of $\frac{\tau^*}{\tau_0}$ for different values of α is shown in Fig. 8. The experimental values of $-\left(\frac{\partial V_a}{\partial \tau^*} \right) \frac{\tau^*}{\tau_0}$ for different values of $\frac{\tau^*}{\tau_0}$ (corrected for change in shear modulus with temperature) are also plotted on the same figure, indicating the right order of magnitude of the experimental results.

VII. ACTIVATION ENERGY OF PAIRS OF KINKS

The apparent activation energy for nucleation of pairs of kinks is

defined as:

$$Q_{\tau}^* = \frac{32\pi\gamma}{3 \left(\frac{1}{K^2} \right)^{1/3}} \quad (13)$$

The apparent activation energy for nucleation of pairs of kinks at 0°K can be determined by the change in strain rate due to the change in temperature at constant stress (τ^*).

$$\dot{\gamma} = \dot{\gamma}_0 e^{-\frac{U_0}{K\tau}}$$

where:

$$\dot{\gamma}_0 = \rho ab \frac{J}{2\pi\lambda} v$$

at the critical temperature (where $\tau^* = 0$).

$$\dot{\gamma}_1 = \dot{\gamma}_0 e^{-\frac{2U_K(\tau_{c1})}{K\tau_{c1}}}$$

$$\dot{\gamma}_2 = \dot{\gamma}_0 e^{-\frac{2U_K(\tau_{c2})}{K\tau_{c2}}}$$

since $\dot{\gamma}_0$ remains constant for both cases,

$$\frac{\dot{\gamma}_2}{\dot{\gamma}_1} = \frac{\exp \left(-\frac{2U_K(\tau_{c2})}{K\tau_{c2}} \right)}{\exp \left(-\frac{2U_K(\tau_{c1})}{K\tau_{c1}} \right)} = \frac{\exp \left(-\frac{2U_K(0)}{K\tau_{c2}} \right) \cdot \frac{2U_K(0)}{K\tau_{c2}} \cdot \frac{G(\tau_{c2})}{G(0)}}{\exp \left(-\frac{2U_K(0)}{K\tau_{c1}} \right) \cdot \frac{2U_K(0)}{K\tau_{c1}} \cdot \frac{G(\tau_{c1})}{G(0)}}$$

or

$$2U_K(0) = \frac{K G(0)}{G(\tau_{c1}) - G(\tau_{c2})} \ln \frac{\dot{\gamma}_2}{\dot{\gamma}_1} \quad (14)$$

Substituting:

$$K = 1.38 \times 10^{-16} \text{ ergs/}^\circ\text{K}$$

$$G(0) = 1.74 \times 10^{10} \text{ dynes/cm}^2$$

$$G(\tau_{c1}) = 1.63 \times 10^{10} \text{ dynes/cm}^2$$

$$G(\tau_{c2}) = 1.56 \times 10^{10} \text{ dynes/cm}^2$$

$$\tau_{c1} = 115^\circ\text{K}$$

$$\tau_{c2} = 160^\circ\text{K}$$

$$\ln \frac{\dot{\gamma}_2}{\dot{\gamma}_1} = 4.602$$

$$2U_K(0) = 0.2 \times 10^{-12}$$

$$= 2 \times 10^{-13} \text{ ergs} = 0.13 \text{ eV}$$

This value is of the right order of magnitude for activation energy, when the rate controlling mechanism is by nucleation of pairs of kinks.

VII. LINE TENSION OF DISLOCATION STUCK AT THE POTENTIAL VALLEY

Sum and Rabinak gave the theoretical values of $\frac{\tau_{ab}}{\tau_0}$ and $\frac{\sigma_{ab}}{\sigma_0}$ for different values of α and β , where $\beta = \frac{\tau_0}{\sigma_0}$ the ratio of the energy at the top and at the bottom of a Peierls hill. The theory demands that:

$$\frac{2\tau_{ab}(0)}{\sigma_0} = 6.49 \sqrt{\beta - 1}$$

$$\frac{\tau_{ab}}{\tau_0} = 1.3 (\beta - 1)$$

$$\frac{2\tau_{ab}(0)}{\sigma_0} = 5.75 \left[\frac{\tau_{ab}}{\tau_0} \right]^{1/2} \quad (15)$$

for $\beta = 1$, where

$$a = b = 3.04 \times 10^{-2} \text{ cm}$$

$$2\tau_{ab}(0) = 0.2 \times 10^{-12} \text{ erg/cm}$$

$$\tau_0 \text{ (extrapolated)} = 6.40 \times 10^8 \text{ dynes/cm}^2$$

Substituting for τ_0 , $\tau_0 = 0.54 \times 10^{-14}$ dynes. The line tension of the dislocation is related to the shear modulus G and the Burger's vector b by the equation:

$$\tau_0 = 65(0)b^2 \quad (16)$$

hence,

$$b = 3$$

This value compared with Nabarro's estimation of the line tension $\frac{Gb^2}{2}$ proves to be of the right order of magnitude.

VIII. EXPERIMENTAL VALUE OF THE NUMBER OF DISLOCATIONS PER UNIT LENGTH (ρ_L)

For a given strain rate and temperature, the value of ρ_L can be determined from the equation.

$$\dot{\gamma} = \frac{\sigma \rho_L b v}{2\pi} e^{-\frac{U^*}{kT}} \quad (17)$$

The Debye frequency was estimated to be 5×10^{12} per sec from the Debye characteristic temperature of magnesium-lithium alloy. Estimating v_0 to be 600 from Fig. 6 and substituting the values of a , b , $2U^*$ and τ_0 , it was found that $\rho_L = 0.3$ per cm. This value of ρ_L seems to be somewhat low when compared with that of Ag_3Zn_9 (227 per cm) and τ_0 (104 per cm).

There are some possibilities that might account for this low value of the number of mobile dislocations per unit length (ρ_L). An obvious possibility is that the preexponential expression of Eq. (17) is somewhat in doubt since v is not well-defined. This arises because the kinks of the critical pair are not abrupt. Another possibility is that the precipitates and impurities could pin-down the dislocation line, modifying the expansion of the kinks by affecting L and v , as qualitatively considered by Kosevsky and Brown. The theory neglects the effects that arise in dislocation segments of finite length which may be restrained at their terminal points on the slip plane. Nevertheless, it is a possible number in terms of the possibility of a low value of L .

IX. CONCLUSIONS

- (1) The strong temperature dependence of the flow stress below 1150°C can be explained by the Dorn and Rajnak theory of the Peierls mechanism of plastic deformation. Above about 1150°C an athermal mechanism is operative.
- (2) The shape of the Peierls humps for magnesium, 14 wt.% Li, 1.5 wt.% Al alloy seems to approach the theoretically predicted curve with $\alpha = -1$.
- (3) The activation energy of the process of the nucleation of pairs of kinks is estimated to be 0.13 eV, which is of the right order of magnitude for activation energy, when the rate-controlling mechanism is by nucleation of pairs of kinks.
- (4) The experimentally deduced values of the apparent activation volume and the line tension are in agreement with the theory.

APPENDIX I

Various authors, Celli et al.,¹⁹ Friedel,²⁰ Jdsseang et al.,²¹ Seeger et al.,²² have described the formulation of the forward velocity of dislocations and the strain rate resulting from the nucleation of pairs of kinks (see Brailsford (1961) regarding the redistribution of existing kinks along a dislocation due to the action of a stress). Only a first order approximation was attempted by P. Guyot and J. Dorn (1966). In (Fig. 1) was assumed to be the average length of a dislocation that might be swept out by a pair of kinks following their nucleation. L was also assumed to be much larger than w , the width of the critical pair of kinks, and end effects were neglected. One possible formulation was based on the fact that there are L/b (b is the Burger's vector) points along the length L at which a pair of kinks might be produced and consequently,

$$v_n = v_D \frac{L}{2b} e^{-\frac{U_n}{kT}} \quad (\text{A.I.1})$$

where v_D is the Einstein frequency. This would apply for cases where the fluctuation might be localized. On the other hand when the thermal fluctuation is spread over the critical width, w , of the pair of kinks,

$$v_n = \frac{v_D}{w} \frac{L}{2b} e^{-\frac{U_n}{kT}} \quad (\text{A.I.2})$$

where v_D/w is the frequency of vibration of the dislocation, v is the Debye frequency, and $\frac{L}{2b}$ is approximately the number of wave lengths along the dislocation line at which nucleation might occur. These expressions

differs somewhat from the original suggestion of Dorn and Rajnak (1964)

(which was based partly on both concepts) that

$$v_n = \frac{2}{\pi} \frac{1}{b} e^{-\frac{U_n}{kT}} \quad (\text{A.I.3})$$

an exact analysis for v_n is quite complicated. Inasmuch as the vibrations are coupled, it appears that Eq. (A.I.2) might prove to be the more satisfactory approximation in most cases. These equations apply only when the velocity of the kinks is so great relative to their nucleation rate that not more than one pair of kinks exist in length L at any one time. Dorn and Rajnak (1964) have also described cases where the kink velocity might be so slow relative to the nucleation rate that several pairs of kinks will be moving along a single dislocation segment at one time. Thus far, however, there have been no experimental confirmations of this possibility.

The average velocity of a dislocation moving as a result of nucleation of pairs of kinks is

$$v = v_n = \frac{v_n}{2} e^{-\frac{U_n}{kT}} \quad (\text{A.I.4})$$

and this gives a shear strain rate of

$$\dot{\gamma} = \rho b v = \frac{\rho L a^2}{2\pi^2} v e^{-\frac{U_n}{kT}} \quad (\text{A.I.5})$$

where b is the total length of all thermally activatable dislocation segments per unit volume of the crystal.

ACKNOWLEDGEMENT

The author is most grateful for the interest and guidance from Professor J. E. Dorn. I also wish to thank Mr. Jack Mitchell for the helpful discussions during the course of this work.

This research was done under the auspices of the United States Atomic Energy Commission.

REFERENCES

1. J. E. Dorn and S. Rajnak, *Trans. AIME*, **230**, 1092 (1964).
2. H. Conrad, "Yielding and Flow of the BCC Metals at Low Temperature", Symposium on the Relation between Structure and Properties of Metals, National Physical Laboratory, Teddington, England (1962).
3. J. H. Christian and B. S. Masters, *Proc. Roy. Soc., A*, **281**, 240 (1964).
4. A. Rosen and J. E. Dorn, *Trans. AIME*, **230**, 1065 (1964).
5. P. Murty, A. Rosen and J. E. Dorn, *Trans. AIME*, **233**, 652 (1965).
6. Pierre Gayot and J. E. Dorn, *CORD-16092*, July, 1966.
7. J. Trivelpiece and Charles S. Smith, *Acta Met.*, **9** [12] Dec. (1961).
8. J. E. Dorn and J. B. Mitchell, *High Strength Materials*, Ed. V. Zackay, John Wiley and Sons, Inc., 510-77 (1965).
9. A. K. Mukherjee and J. E. Dorn, *Trans. AIME*, **230**, 1065 (1964).
10. A. K. Cottrell, Rpt. on the Strength of Solids, *Phys. Soc.*, London, p. 30 (1946); Conference on High Rates of Strain, *Inst. Mech. Eng.* London, p. 448.
11. A. K. Cottrell and B. A. Bilby, *Proc. Phys. Soc.*, **62A**, 49 (1949).
12. J. C. Fischer, *Trans. ASM*, **47**, 451 (1955).
13. H. F. Lotz, *Proc. Phys. Soc.*, **B69**, 454 (1956); *ibid.* **B71**, 444 (1958).
14. G. Schoeck, *Acta Met.*, **9**, 382 (1961).
15. J. A. Rose, D. P. Ferris and J. Muller, *Trans. AIME*, **224**, 901 (1962).
16. E. L. Korzikke, *Zeit. f. Metall.*, **52**, 586 (1962).
17. E. L. Korzikke and P. Hassen, *Phil. Mag.*, **7**, 459 (1962).
18. H. Brown and R. A. Ekvall, *Acta Met.*, **10**, 1101 (1962).
19. T. Kamiya, M. Kato, T. Minamiya and R. Thomson, *Phys. Rev.*, **131**,

58 (1963).

20. J. Friedel, NPL Conference, Teddington, England (1963); *Dislocations*, Pergamon Press (1964).
21. T. Gjessing, K. Skjeltved, and J. Lotke, NPL Conference, Teddington, England (1963).
22. A. Seeger, H. Dorn, and F. Pfaff, *Discussion Faraday Soc.*, **22**, 19 (1957).
23. R. Kossovsky and N. Brown, Technical Report of the University of Pennsylvania Laboratory for Research on the Structure of Matter, March 30, 1965.
24. S. Lee, private communication.

FIGURE CAPTIONS

- Figure 1. Schematic diagram showing the nucleation of a pair of kinks. a is the spacing between parallel rows of closely spaced atoms of the slip plane.
- Figure 2. 0.05% flow stress, τ , vs. temperature.
- Figure 3. The thermally activated 0.05% flow stress, τ^* , vs. temperature.
- Figure 4. Variation of shear modulus G with temperature.
- Figure 5. The thermally activated component of the flow stress vs. temperature in dimensionless units.
- Figure 6. The thermally activated component of the flow stress vs. the activation volume in units of b^3 .
- Figure 7. Apparent activation volume at $77^\circ K$ vs. strain.
- Figure 8. The thermally activated component of the flow stress vs. activation volume in dimensionless units.

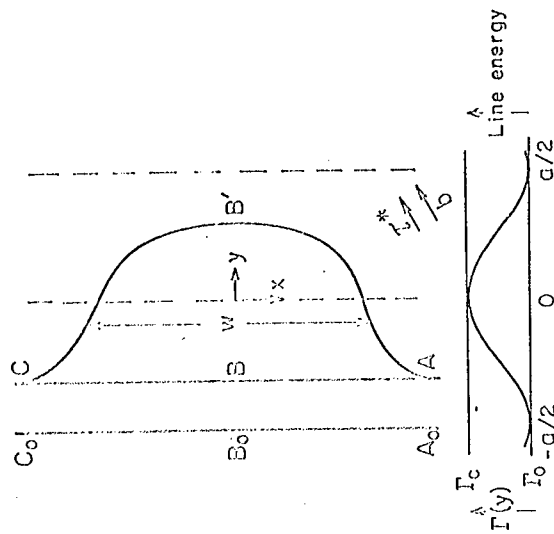


FIG. 1 NUCLEATION OF A
PAIR OF KINKS.

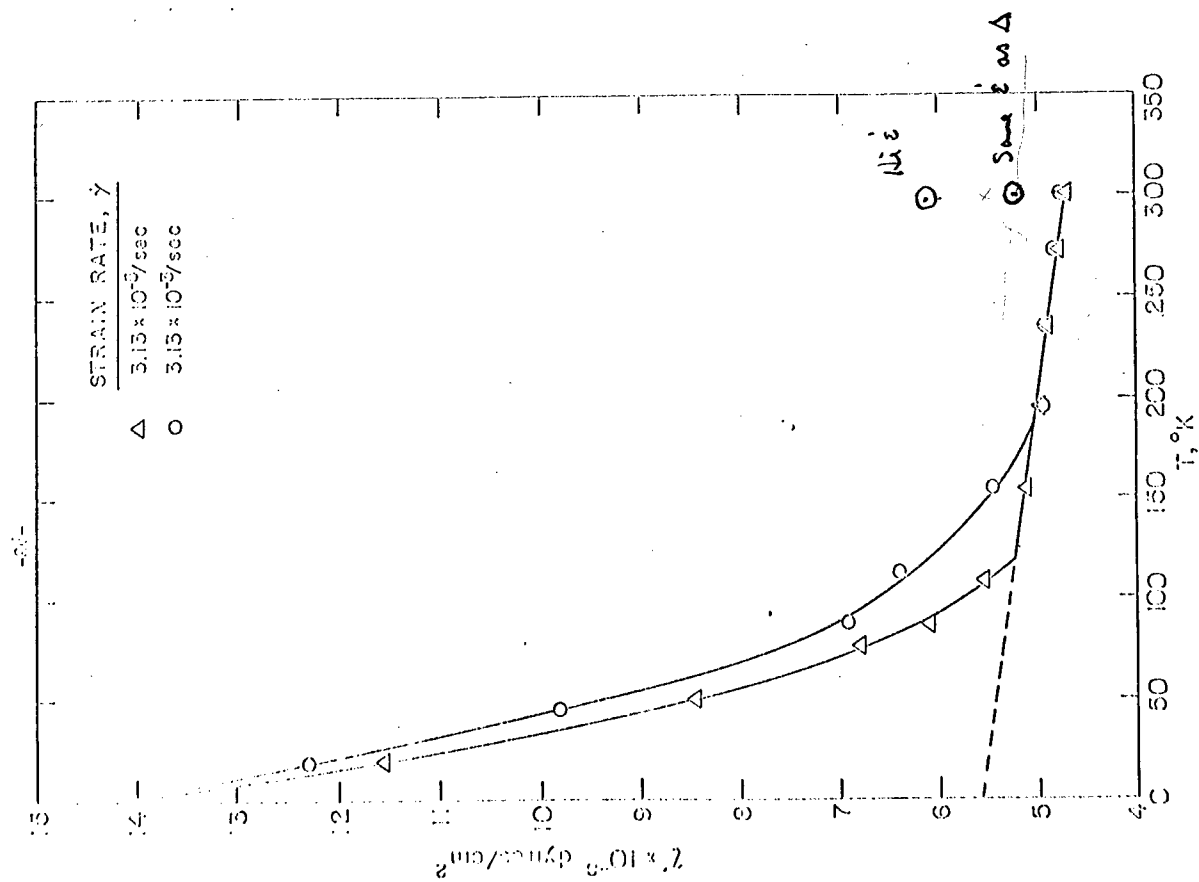


FIG. 2 0.05% FLOW STRESS vs TEMPERATURE.

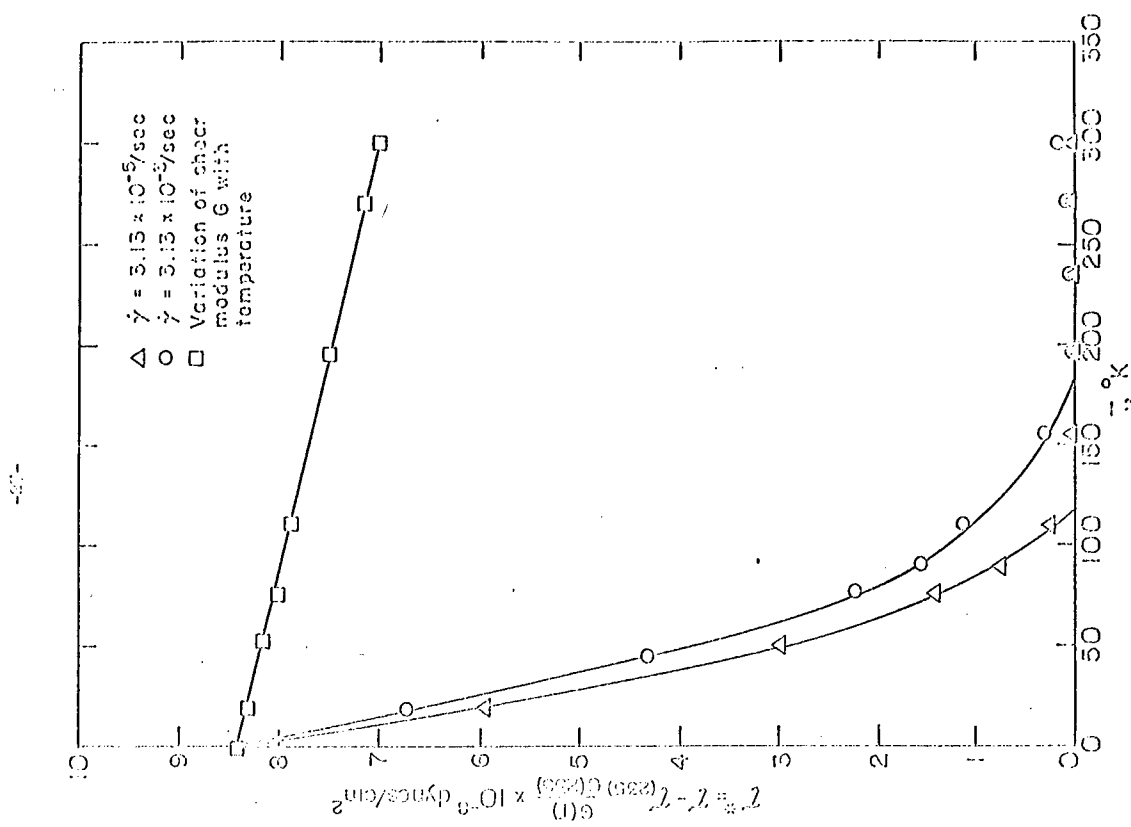
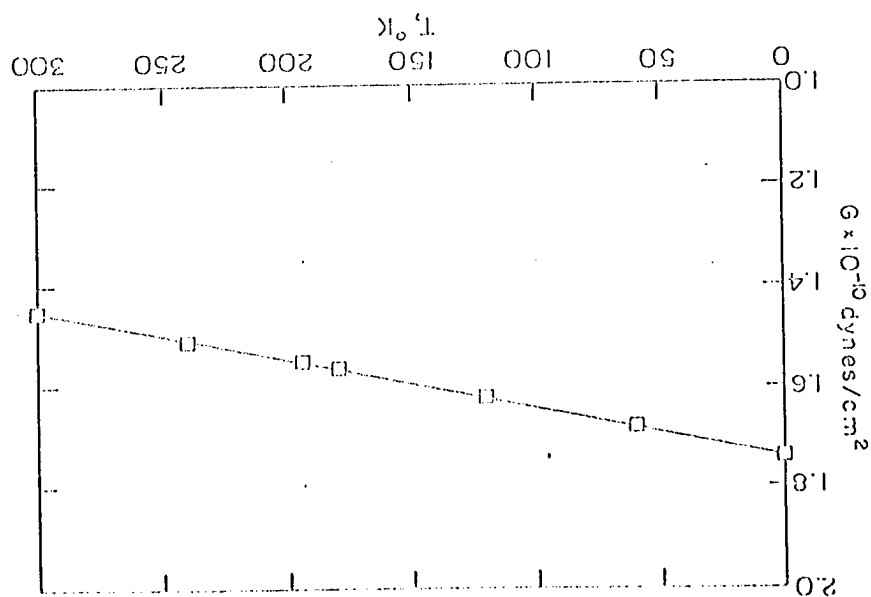


FIG. 3 THERMALLY ACTIVATED 0.05% FLOW STRESS vs TEMPERATURE.

FIG. 4 VARIATION OF SHEAR MODULUS G WITH TEMPERATURE.



-2-

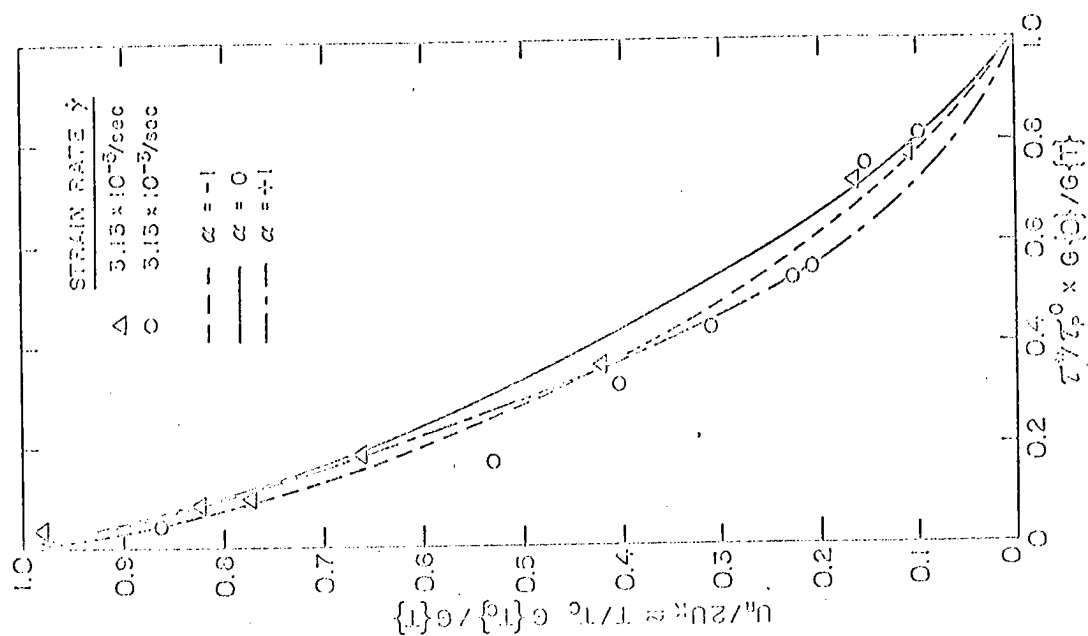


FIG. 5 THE THERMALLY ACTIVATED COMPONENT OF THE FLOW STRESS VS TEMPERATURE IN DIMENSIONLESS UNITS.

FIG. 7 APPARENT ACTIVATION VOLUME AT 77°K vs STRAIN.

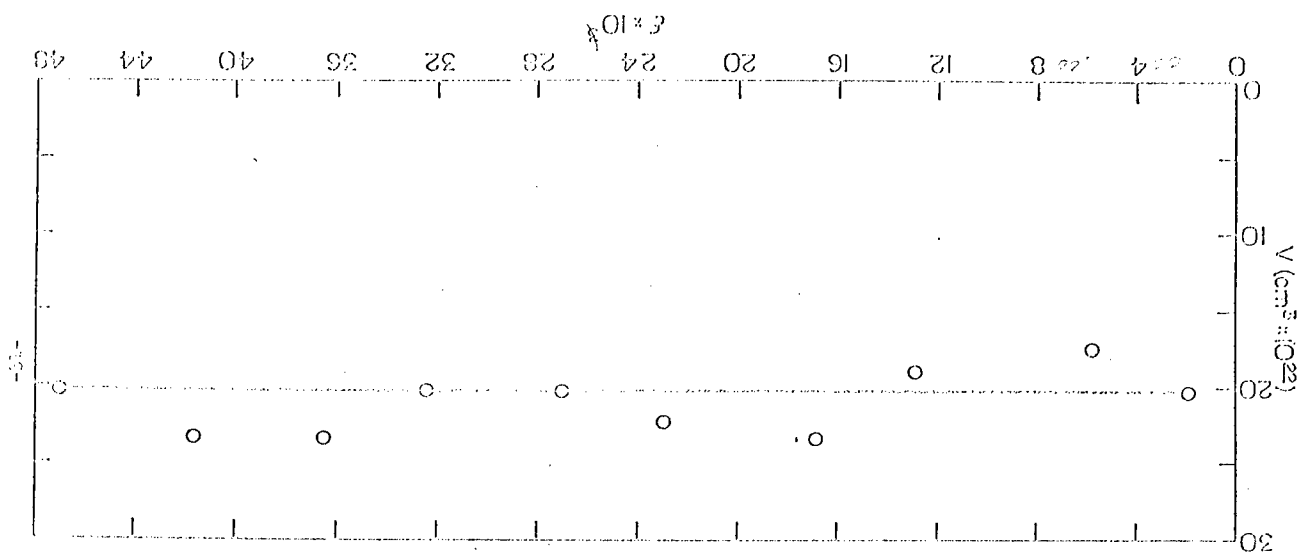


FIG. 6 THE THERMALLY ACTIVATED COMPONENT OF THE FLOW STRESS vs THE ACTIVATION VOLUME IN UNITS OF b^3

$$\text{Corrected } V(b^3) \times 4.3 = \text{corrected } V(b^3)$$

